Mass property estimation by EKF and UKF for spacecraft

Keisuke Sugawara[1)], Matthew M. Wittal[2)], Yoshinori Kondoh[1)], Yu Nakajima[1)]

[1)]*Japan Aerospace Exploration Agency, Japan;* [2)]*National Aeronautics and Space Administration, US*

(Received March 10th, 2025)

The Lunar Gateway is a manned spacecraft being constructed in a near-rectilinear halo orbit around the Moon. Such projects require supply chains in order to sustain human presence and, by extension, a spacecraft which can transport cargo. Unlike common satellites, these spacecrafts have different mass properties for every mission depending on their cargo and can even have different mass properties during the same mission as cargo is loaded and unloaded during docking. Thus, if the mass properties can be estimated on orbit, human resources and fuel can be significantly reduced through the use of effective control.

As a first step toward this goal, this work presents simulation results of a mass property estimation method with the intent to use on orbit. A simulation environment for JAXA's HTV-X resupply vehicle to the International Space Station was designed. Two methods were tested: an Extended Kalman Filter (EKF)-based method and an Unscented Kalman Filter (UKF)-based method, both of which estimate center of mass and all 6 elements of the inertia tensor simultaneously and in addition to state vectors which consist of attitude and angular velocity.

These two methods were evaluated using simulation data. As a result, the EKF estimated center of mass with less than 1.3 cm accuracy and diagonal elements of inertia matrix with less than 0.8% accuracy. The UKF estimated center of mass within 2.2 cm. accuracy and inertia matrix with 1.2% accuracy. The computational load of the EKF was compared to the UKF and EKF was executed 91% faster. These results demonstrate two robust methods of estimating complete mass properties in the presence of process, measurement, and thruster noise.

Key Words: Spacecraft, Mass property estimation, Extended Kalman filter, Unscented Kalman filter

Nomenclature

$\boldsymbol{q}$	:	attitude quaternion
$\boldsymbol{\omega}$	:	attitude rate, rad/s
$\mathbf{I}$	:	inertia matrix
$\boldsymbol{\tau}$	:	torque, N·m
s_n	:	true force of n-th thruster [N]
u_n	:	on/off control signal of n-th thruster
$\boldsymbol{r_n}$	:	position of n-th thruster, [m] (gap with center of mass)
$\boldsymbol{d}_n$	:	orientation of n-th thruster (normalized)
$\overline{\boldsymbol{q}_k}$	:	observation value of attitude quaternion by star tracker
$\overline{\boldsymbol{\omega}_k}$	:	observation value of attitude rate by gyro sensor, [rad/s]
s'	:	rating force of a thruster [N]
s''	:	random noise of thruster force [N]
Δt	:	simulation timestep [seconds]

1. Introduction

1.1. Background

Many spacecrafts have constant mass properties, or mass properties that vary only as a function of fuel depletion. The system parameters required for estimating their attitude by using a Kalman filter or other method are set in advance on the ground based on identified values. On the other hand, some spacecraft have mass properties that change from one mission phase to another. For example, among space station supply ships, those that carry waste from the space station have mass properties that change before and after loading. Satellites that capture space debris in orbit also have mass properties that change before and after capture, and planetary sample return missions must reevaluate mass properties following sample acquisition.

HTV-X is a cargo spacecraft designed for International Space Station (ISS) resupply missions currently under development by JAXA. A simplified mission sequence is shown in Fig. 1. After resupplying the ISS with supplies, waste from inside the ISS is loaded onto the vehicle, which then re-enters the atmosphere. In order to ensure proper control, astronauts must place specific cargo in specific locations so that the entire HTV-X aircraft complies with predetermined mass property constraints when loading waste. This operation is very demanding on both crew and ground support team, taking many hours to complete. If cargo can be placed randomly and the mass properties of the spacecraft can be estimated in orbit, it may be possible to significantly reduce crew time.

1.2. Problem Statement

Based on the above problems, this paper proposes a method for estimating the mass properties, center of mass and inertia tensor, of the HTV. These mass properties are necessary for estimating attitude, and conversely, attitude values are necessary for estimating mass properties. We propose a method for estimating attitude, attitude rate, and mass properties simultaneously using a Kalman filter.

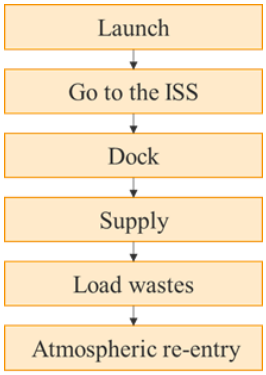

Fig. 1. A simplified mission sequence of HTV-X.

In this paper, a simulation environment that simulates the dynamics of HTV-X and evaluates the proposed method in that environment has been constructed. We applied the proposed method to two types of methods: the Extended Kalman Filter (EKF) and Unscented Kalman Filter (UKF), and compared their performance. The proposed method demonstrated high accuracy in estimating mass properties for simulation data. In particular, the center of mass position was estimated with an error of about 7.46 mm using EKF. Currently, the method has only been demonstrated to be effective for simulation data, but it is expected to be applicable to actual vehicle data in the future.

1.3. Related work

Numerous methods have been proposed for estimating the mass properties of spacecraft. Ref. 1) estimated the center of gravity and moment of inertia using a method similar to EKF. In this paper, we add attitude and attitude rate to the state variable and simultaneously estimating attitude and attitude rate.

There are also cases where mass properties have been estimated in actual missions. Ref. 2) estimated change in the moment of inertia before and after sample collection in the OSIRIX-REx mission. Ref. 3), examines changes in moments angular momentum vector before and after sample acquisition to deduce changes in mass for the same mission, which was the actual method employed.

As shown in ref. 4), the state of a spacecraft is expressed using a Lie group, and its mass properties are estimated. The attitude, position and their differential of the spacecraft are expressed as an element of the Lie group. The advantage of this approach is that it allows simultaneous handling of translational and rotational motions. The benefit is that this method estimates total mass in addition to center of mass and moments of inertia, and has been shown to be quite accurate in an analogous simulation. The disadvantage is that a more robust measurement model is needed. In addition, an increase in the number of estimated variables means an increase in the dimension of the state space, which makes it more difficult to design estimation methods. Therefore, we first demonstrate the estimation of only the center of mass and moment of inertia among the mass properties, and then proceed to the estimation of mass. In the future, we will consider introducing the concept of Lie groups.

Methods for estimating system parameters can be divided into two categories in terms of the simultaneity of estimation. One method, as in this study, expresses the motion state of the system, such as the attitude and attitude rate of a spacecraft, and the static parameters of the system as state variables, and estimates them simultaneously. Another method, as shown in ref. 5), handles them as separate variables and estimates them sequentially while fixing one of them.

In this study, we evaluate the proposed method by using simulation data. We assume that the thrust error of the thruster follows a normal distribution, but the thrust of the thruster in actual orbit is not thought to follow a simple normal distribution, and this may have a significant impact on the accuracy of the mass property estimation, thus further investigation is needed. Ref. 6) propose a model that can accommodate the uncertainty of the thruster thrust.

2. Preliminaries

2.1. Dynamics data

As a first step, the performance of the proposed method using a simulator is evaluated. In this chapter, we describe the simulator model.

We assume a spacecraft system that simulates HTV-X. The Table 1, Table 2, Table 3 and Table 4 shows the sensors and actuators that compose the system. Note that this is a model of satellite parameters and differs from actual design values. Attitude changes are performed by thrusters. The thruster operation signals are given at each time k by vector $\mathrm{u}_k \in \{0,1\}^8$. There are eight thrusters, each with its own bias and uniform random noise. That is, the rated force of the thrusters is 125 N, but the actual force at each time when the operation signal is 1 is subject to noise following a normal distribution shown in Table 2. The mean is set based on a normal distribution with standard deviation 6.25 [N] and mean of 0 ($\mathcal{N}\sim(0,6.25\ [N])$ for each thruster, and this is time-invariant. Table 3 and Table 4 show mounting position and orientation of thrusters, and their assumed and true values. The true value of the thruster mounting position is a value with noise following a normal distribution with a mean of 0 and a standard deviation of 0.01 [m] added to the assumed value. The true value of the thruster orientation is a value with noise following a normal distribution with a mean of 0 and a standard deviation of 1.0 [degree] added to the assumed value.

The state equations representing the rotational motion of the spacecraft system are as follows.

$$\dot{\boldsymbol{q}} = \frac{1}{2}\tilde{\boldsymbol{\omega}}\boldsymbol{q}$$

$$\mathbf{I}\dot{\boldsymbol{\omega}} + \tilde{\boldsymbol{\omega}}\mathbf{I}\boldsymbol{\omega} = \boldsymbol{\tau}$$

Where $\mathbf{I}$ is inertia tensor and $\boldsymbol{\tau}$ is torque vector. $\boldsymbol{q}$ is quaternion and $\boldsymbol{\omega}$ is attitude rate,

$$\mathbf{I} = \begin{bmatrix} I_{xx} & I_{xy} & I_{zx} \\ I_{yx} & I_{yy} & I_{yz} \\ I_{zx} & I_{zy} & I_{zz} \end{bmatrix}, \boldsymbol{q} = \begin{bmatrix} q_0 \\ q_1 \\ q_2 \\ q_3 \end{bmatrix}, \boldsymbol{\omega} = \begin{bmatrix} \omega_x \\ \omega_y \\ \omega_z \end{bmatrix}$$

$\tilde{\boldsymbol{\omega}}$ is a tilde matrix of $\boldsymbol{\omega}$,

$$\tilde{\boldsymbol{\omega}} = \begin{bmatrix} 0 & \omega_z & -\omega_y & \omega_x \\ -\omega_z & 0 & \omega_x & \omega_y \\ \omega_y & -\omega_x & 0 & \omega_z \\ -\omega_x & -\omega_y & -\omega_z & 0 \end{bmatrix}$$

In this study, no external forces other than thruster thrust acting on the spacecraft during rotational motion are considered. For example, gravitational inclination, atmospheric drag, and solar radiation pressure are excluded. Therefore, $\boldsymbol{\tau}$ is a torque by thruster force.

$$\boldsymbol{\tau} = \mathbf{M} \begin{bmatrix} s_0 u_0 \\ s_1 u_1 \\ \vdots \\ s_7 u_7 \end{bmatrix}$$

Where $\mathbf{M} \in \mathbb{R}^{3\times 8}$ is the momentum action matrix of 8 thrusters,

$$\mathbf{M} = [\boldsymbol{r}_0 \times \boldsymbol{d}_0 \quad \boldsymbol{r}_1 \times \boldsymbol{d}_1 \quad \cdots \quad \boldsymbol{r}_7 \times \boldsymbol{d}_7]$$

$$\boldsymbol{r}_n \times \boldsymbol{d}_n = \begin{bmatrix} 0 & -(p_{n,z} - c_z) & p_{n,y} - c_y \\ p_{n,z} - c_z & 0 & -(p_{n,x} - c_x) \\ -(p_{n,y} - c_y) & p_{n,x} - c_x & 0 \end{bmatrix} \boldsymbol{d}_n$$

Where $\boldsymbol{r}_n$ is n-th thruster's mounting position at body-fixed frame. $\boldsymbol{d}_0$ is normalized n-th thruster's orientation vector at body-fixed frame. $\boldsymbol{c}$ is spacecraft's center of mass and $\boldsymbol{p}_n$ is n-th thruster's point of effort at body-fixed frame,

$$\boldsymbol{c} = [c_x \quad c_y \quad c_z]^{\mathrm{T}}$$

$$\boldsymbol{p}_n = [p_{n,x} \quad p_{n,y} \quad p_{n,z}]^{\mathrm{T}}$$

And s_n is a true force of n-th thruster and follow a normal distribution whose parameter is shown in Table 2.

Table 1. Sensors list.

Sensor Type	Physical quantity	Uncertainty
Star Tracker	Attitude	X: $\mathcal{N}(0, 1.53)$ [arcsec] Y: $\mathcal{N}(0, 1.53)$ [arcsec] Z: $\mathcal{N}(0, 15.3)$ [arcsec]
Gyroscope	Attitude rate	Variance-covariance matrix: $1.0 \times 10^{-5} \begin{bmatrix} 1 & 0 & 0 \\ 0 & 1 & 0 \\ 0 & 0 & 1 \end{bmatrix}$ [rad/s]

Table 2. Thruster force uncertainty.

Index	Uncertainty [N]
#0	$\mathcal{N}(124.97, 6.25)$
#1	$\mathcal{N}(125.01, 6.25)$
#2	$\mathcal{N}(124.92, 6.25)$
#3	$\mathcal{N}(125.05, 6.25)$
#4	$\mathcal{N}(124.98, 6.25)$
#5	$\mathcal{N}(125.01, 6.25)$
#6	$\mathcal{N}(125.01, 6.25)$
#7	$\mathcal{N}(125.00, 6.25)$

Table 3. Assumed and true mounting position of thrusters

	Assumed mounting position [m]	True mounting position [m]
#0	[0.100 1.67 −1.27]	[0.0875 1.67 −1.27]
#1	[0.100 1.67 1.27]	[0.899 1.68 1.29]
#2	[0.100 −1.67 1.27]	[0.0909 −1.6685 1.25]
#3	[0.100 −1.67 −1.27]	[0.0974 −1.69 −1.25]
#4	[0.300 1.67 −1.27]	[0.300 1.68 −1.25]
#5	[0.300 1.67 1.27]	[0.311 1.66 1.26]
#6	[0.300 −1.67 1.27]	[0.302 −1.69 1.28]
#7	[0.300 −1.67 −1.27]	[0.295 −1.67 −1.25]

Table 4. Assumed and true orientation of thrusters

	Assumed orientation	True orientation
#0	[0.864 −0.264 0.428]	[0.865 −0.263 0.428]
#1	[0.864 −0.264 −0.428]	[0.865 −0.256 −0.436]
#2	[0.864 0.264 −0.428]	[0.865 0.263 −0.428]
#3	[0.864 0.264 0.428]	[0.864 0.267 0.428]
#4	[−0.864 −0.264 0.428]	[−0.862 −0.262 0.434]
#5	[−0.864 −0.264 0.428]	[−0.868 −0.260 −0.423]
#6	[−0.864 0.264 −0.428]	[−0.867 0.261 −0.424]
#7	[−0.864 0.264 0.428]	[−0.861 0.270 0.431]

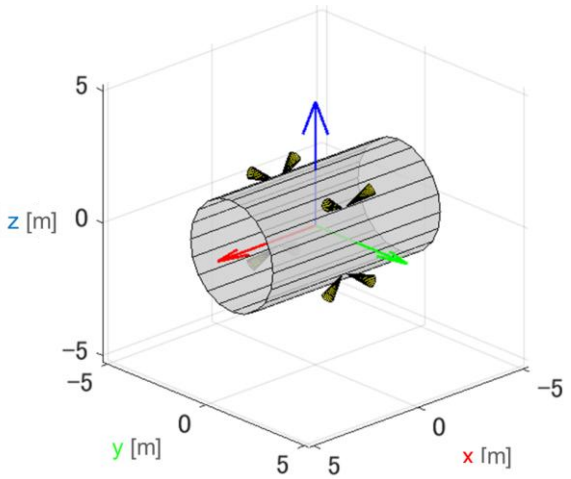

Fig. 2. Thruster position and orientation of HTV-X. The gray cylinder represents the HTV-X body. Yellow cones, 6 are visible and 2 are hidden behind the body, are the thrusters on the HTV-X body. X-Y-Z axis are body-fixed frame.

2.2. Mass property data

Table 5 shows the truth and initial estimation value of center of mass and inertia tensor elements. Initial estimation value is given to the EKF and UKF, then used as initial estimation value. Note that this is a model of satellite parameters and differs from actual design values.

Table 5. truth and initial estimation value of mass property

	Truth	Initial estimation
Center of mass X [m]	-0.06	0.94
Center of mass Y [m]	0.1	-0.65
Center of mass Z [m]	-0.2	-0.1
Inertia I_{xx} [kg · m^2]	37510	38510
Inertia I_{yy} [kg · m^2]	19000	20000
Inertia I_{zz} [kg · m^2]	19000	20000
Inertia I_{xy} [kg · m^2]	0	100
Inertia I_{yz} [kg · m^2]	0	200
Inertia I_{zx} [kg · m^2]	0	300

2.3. Methods

We define state variable as 16 dimensions vector.

$$\boldsymbol{x}_k = \begin{bmatrix} \boldsymbol{q}_k \\ \boldsymbol{\omega}_k \\ \boldsymbol{c} \\ I_{xx} \\ I_{yy} \\ I_{zz} \\ I_{xy} \\ I_{yz} \\ I_{zx} \end{bmatrix}$$

They are composed of quaternion, attitude rate, center of mass and inertia matrix elements. And observation variable as 7 dimensions vector.

$$\boldsymbol{y}_k = \begin{bmatrix} \overline{\boldsymbol{q}_k} \\ \overline{\boldsymbol{\omega}_k} \end{bmatrix}$$

And equation of state is shown as this,

$$\begin{cases} \boldsymbol{x}_{k+1} = f_k(\boldsymbol{x}_k, \boldsymbol{u}_k) + \boldsymbol{w}_k \\ \boldsymbol{y}_k = h(\boldsymbol{x}_k) + \boldsymbol{v}_k \end{cases}$$

$\boldsymbol{q}_k$ and $\boldsymbol{\omega}_{k+1}$ are updated by this equation. $\boldsymbol{c}$ and $\mathbf{I}$ are not updated.

$$\boldsymbol{q}_{k+1} = \boldsymbol{q}_k + \frac{1}{2}\tilde{\boldsymbol{\omega}}\boldsymbol{q}_k \Delta t$$

Thus, $f_k(\boldsymbol{x}_k)$ in non-linear function. Linear Kalman filter is not able to estimate the state variable. By applying EKF and UKF to this equation of state to estimate the state vector, quaternion, attitude rate and mass property can be estimated simultaneously.

Observation function $h(\boldsymbol{x}_k)$ is a linear function and composed of matrix $\mathbf{H} \in \mathbb{R}^{7\times16}$,

$$\begin{aligned} h(\boldsymbol{x}_k) &= \mathbf{H}\boldsymbol{x}_k \\ &= [\boldsymbol{E}_7 \quad \boldsymbol{O}_{9,9}]\boldsymbol{x}_k \end{aligned}$$

EKF and UKF treat process noise as $\boldsymbol{w}_k$. In this problem setting, thruster force error corresponds to the process noise. We assume thruster force follows normal distribution whose mean is 0 and standard deviation (SD) is $\sigma\boldsymbol{u}_k$. As shown in Table 2, $\sigma = 6.25$ [N]. Variance-covariance matrix of all thrusters $\boldsymbol{\Sigma}$ is a diagonal matrix:

$$\boldsymbol{\Sigma}_k = \begin{bmatrix} \sigma u_{k,0} & \cdots & 0 \\ \vdots & \ddots & \vdots \\ 0 & \cdots & \sigma u_{k,7} \end{bmatrix}$$

And from (3) and (6), the effect of thruster force uncertainty to the chang of attitude late $\Delta\boldsymbol{\omega}$ is

$$\Delta\boldsymbol{\omega} = \mathbf{I}^{-1}\left(\mathbf{M}\begin{bmatrix}(s'+s'')u_0 \\ (s'+s'')u_1 \\ \vdots \\ (s'+s'')u_7\end{bmatrix} - \tilde{\boldsymbol{\omega}}\mathbf{I}\right)\Delta t$$

Thus, change of attitude late follows three-dimensional normal distribution whose mean is $[0,0,0]^{\mathrm{T}}$ and variance-covariance matrix is $\mathbf{I}^{-1}\mathbf{M}\boldsymbol{\Sigma}_k(\mathbf{I}^{-1}\mathbf{M})^{\mathrm{T}}\Delta t^2 \in \mathbb{R}^{3\times3}$. Variance-covariance matrix of process noise in EKF and UKF is expressed $\mathbf{Q} \in \mathbb{R}^{16\times16}$ and,

$$\mathbf{Q}_k = \begin{bmatrix} \sigma_Q & 0 & 0 & & & & & \\ 0 & \ddots & 0 & \boldsymbol{O}_{4,3} & & \boldsymbol{O}_{4,9} & & \\ 0 & 0 & \sigma_Q & & & & & \\ & \boldsymbol{O}_{3,4} & & \mathbf{I}^{-1}\mathbf{M}\boldsymbol{\Sigma}_k(\mathbf{I}^{-1}\mathbf{M})^{\mathrm{T}}\Delta t^2 & & \boldsymbol{O}_{3,9} & & \\ & & & & \sigma_Q & 0 & 0 \\ & \boldsymbol{O}_{9,4} & & \boldsymbol{O}_{9,3} & 0 & \ddots & 0 \\ & & & & 0 & 0 & \sigma_Q \end{bmatrix}$$

Diagonal element of $\mathbf{Q}$ is σ_Q. It is very small value because updating attitude (quaternion) has no uncertainty and mass properties are constant. The value is like 10^{-10} and set at initialization as constant.

And observation noise $\boldsymbol{v}_k$ is also treated. In EKF and UKF, its variance-covariance matrix is expressed as matrix $\mathbf{R} \in \mathbb{R}^{7\times7}$. This value should be determined based on sensor uncertainty. In this paper, this parameter is automatically searched by an exhaustive method.

The simulation flow is shown in the Fig. 3. After initial settings, the torque generated by the actuator in response to the actuator control signals are simulated. Based on this, the rotational dynamics are simulated, and the sensor output is generated using this as the true value. The state variables are estimated using EKF and UKF using this value. Simulation timestep Δt is 0.125 seconds.

The control signals for the thrusters are set to repeat the following motion: the HTV-X spacecraft performs $\pm$X, $\pm$Y, $\pm$Z translations and $\pm$Roll, $\pm$Pitch, $\pm$Yaw rotations for 1 seconds each. By implementing control that ensures uniform motion in all axes, it is expected that sensitivity will be introduced in the estimation of all elements of the inertia tensor and the center of mass positions in all three axes, enabling accurate estimation.

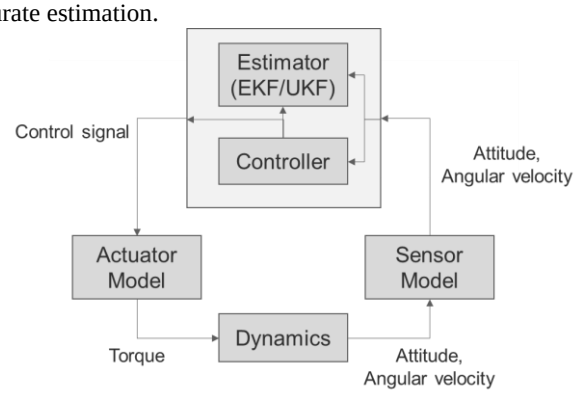

Fig. 3. A simplified simulation sequence.

3. Results

3.1. Hyper parameter search

UKF has three hyperparameter, often listed as α, β, κ, which are used to determine the weights and distribution of the sigma points. First, a Montecarlo search was performed to find the best combination of α, β, κ. The result is shown in Fig. 4. One point means one sample of the combination and center of mass estimation performance. The color of a point whose estimation performance is best when it is green, and the magnitude of the error is inversely proportional to the size of the point after being normalized on the exponential map. Broad trends from the study could not be identified from the provided parameters. The same happened when estimating attitude, attitude rate the moment of inertia matrix. We concluded that initial state covariance $\mathbf{P}_0$, process noise parameter σ_q, observation noise parameter $\mathbf{R}$ are dominating rather than α, β, κ. EKF has also those parameters. Thus, an exhaustive search of these parameters for both EKF and UKF was performed, and estimation performance was quantified.

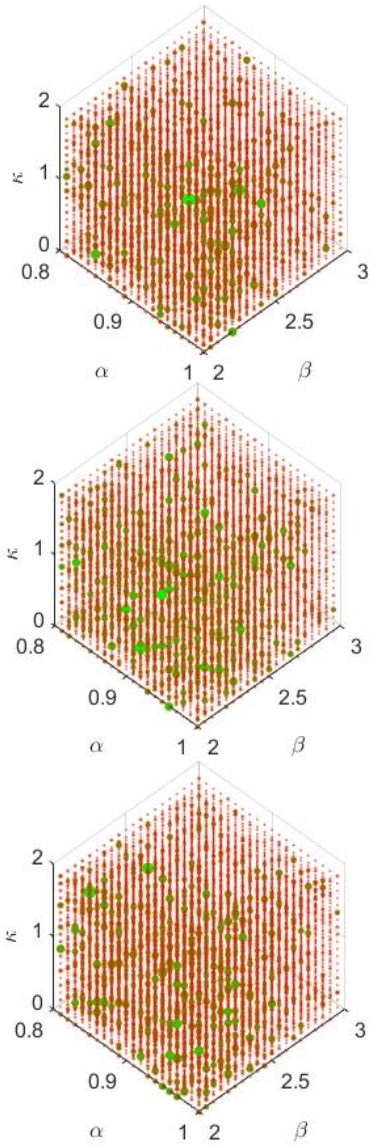

Fig. 4. The result of hyper parameter search of UKF on the estimated Moment of Inertia elements.

3.2. Comparison between EKF and UKF

The performance of mass property estimation was evaluated and compared using EKF and UKF. The absolute values of difference between the true values and estimated values of each state variable after 60 seconds were calculated and shown in Table 6. Time change of each state variable is shown in Fig. 5 to Fig. 8.

EKF was able to estimate attitude and attitude rate with high accuracy. The center of mass position was estimated with an accuracy of less than 0.1 m. The diagonal components of the inertial moment could be estimated with an accuracy of 100 or less. The non-diagonal components I_{xy} converged, but I_{yz} and I_{zx} did not, and the accuracy remained between 1000 and 2000. The UKF attitude rate estimation did not converge, and the error gradually increased. In addition, the inertial moment estimation did not converge, and all of the estimation error were large compared to the EKF.

Table 6. Estimation result of EKF and UKF.

	EKF	**UKF**
Euler angle α [deg]	3.61×10^{-4}	3.51×10^{-4}
Euler angle β [deg]	1.60×10^{-4}	1.48×10^{-4}
Euler angle γ [deg]	2.26×10^{-4}	2.70×10^{-4}
Attitude rate (Roll) [rad/s]	6.40×10^{-5}	5.67×10^{-5}
Attitude rate (Pitch) [rad/s]	1.80×10^{-4}	1.57×10^{-4}
Attitude rate (Yaw) [rad/s]	1.04×10^{-6}	2.78×10^{-5}
Center of mass X [m]	1.25×10^{-2}	2.18×10^{-2}
Center of mass Y [m]	1.94×10^{-4}	1.98×10^{-3}
Center of mass Z [m]	5.76×10^{-3}	3.66×10^{-3}
Inertia I_{xx} [kg · m^2]	28.9	315
Inertia I_{yy} [kg · m^2]	139	218
Inertia I_{zz} [kg · m^2]	25.8	18.7
Inertia I_{xy} [kg · m^2]	15.7	2.44
Inertia I_{yz} [kg · m^2]	57.8	75.3
Inertia I_{zx} [kg · m^2]	79.9	108

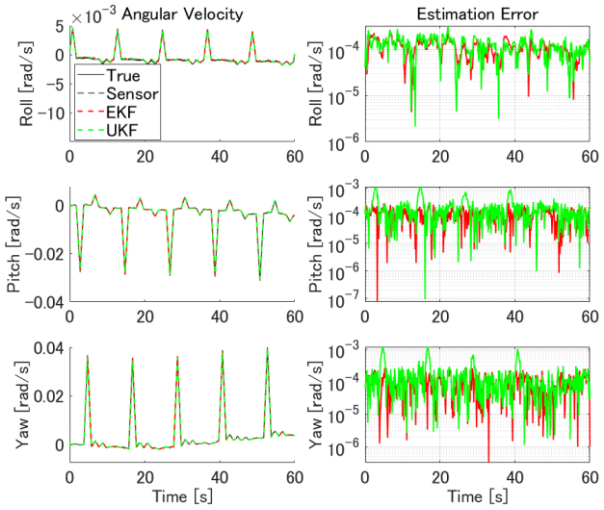

Fig. 5. Left column: Timeseries of true value, sensor value, estimated value of attitude rate. Right column: Estimation error of EKF and UKF.

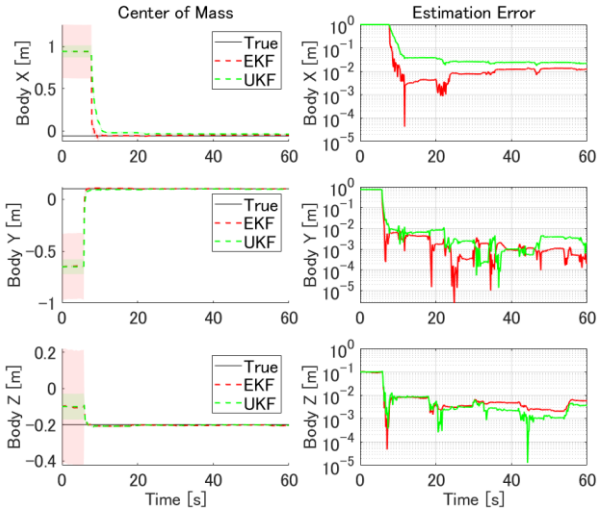

Fig. 6. Left column: True value and timeseries of estimated value of center of mass. Right column: Estimation error of EKF and UKF.

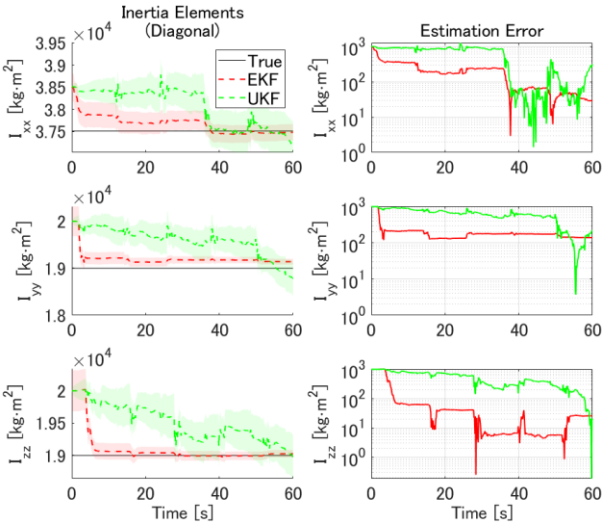

Fig. 7. Left column: True value and timeseries of estimated value of diagonal inertia element. Right column: Estimation error of EKF and UKF.

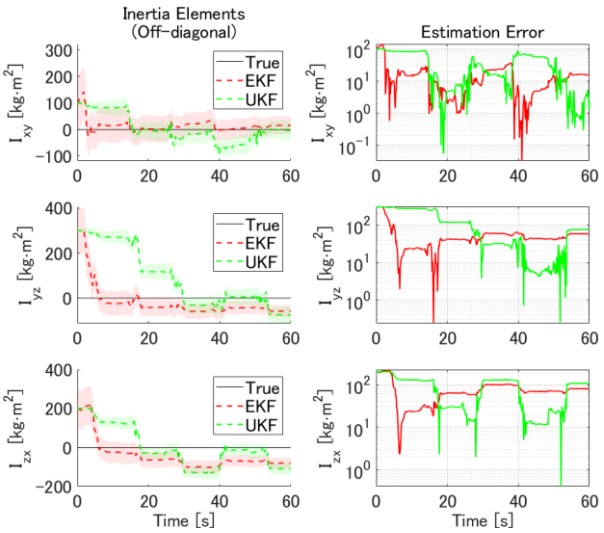

Fig. 8. Left column: True value and timeseries of estimated value of off-diagonal inertia element. Right column: Estimation error of EKF and UKF.

4. Discussion

The EKF was able to estimate mass properties with higher accuracy than the UKF. One reason for the high performance of the EKF is that the nonlinearity of $f_k(\boldsymbol{x}_k, \boldsymbol{u}_k)$ was not very high and sufficient approximation could be obtained even with the Jacobian. Specifically, the highest order of the internal terms of $f_k(\boldsymbol{x}_k, \boldsymbol{u}_k)$ is second order of state variables, thus using the Jacobian as the first-order approximation did not pose significant issues. However, if the thruster mounting position or orientation were also included as state variables, terms of third order or higher would arise, making the Jacobian approximation insufficient and potentially leading to poor performance.

The cause of the UKF estimation error is currently unknown. One possible cause is the difference in the order of magnitude of state variables. The center of mass position is on the order of 10^0, while the diagonal components of the inertia matrix are on the order of 10^4. We are using these without correcting for scaling factors, which may be causing the sigma points to be generated incorrectly and affecting the estimation results.

From the perspective of application, the proposed method can be used for other missions such as sample return and debris capture. From a technical point of view, it is also possible to estimate other system parameters. In this study, we focused on the mass properties among the variables included in the state equation, but if the true force of the thruster is treated as a state variable, it can also be estimated. However, as mentioned above, when nonlinearity of state equation increases, even EKF may not be able to perform accurate estimation.

There are many issues that need to be overcome in order to actually estimate mass properties on orbit. For example, the observation cycle of sensors generally varies depending on the type of sensor. The observation cycle of STTs is often longer than that of gyros. In this study, we assumed that all observation cycles are the same, but we would like to investigate methods that can be used even when they are different. In addition, the computing resources of onboard computers are generally smaller than those on the ground. It is necessary to select an appropriate estimation method by balancing the amount of computation and the estimation accuracy.

5. Conclusion

In this paper, we proposed a method for estimating the center of mass and inertia matrix of HTV-X using EKF and UKF. Using simulation data, we demonstrated that EKF can estimate the center of gravity position with high accuracy of several centimeters. On the other hand, UKF has relatively low estimation accuracy. The anomalous behavior of the UKF is not consistent with other work (ref. 4,5), and needs further analysis and improvement. In the future, the performance of these methods will be evaluated not only using simulation data but also actual telemetry data.

References

1) Bergmann, E. V.: Mass Property Estimation for Control of Asymmetrical Satellites, The AIAA Guidance, Navigation, and Control Conference, Snowmass, CO, 1985
2) Ma, H., Skeen, M., Olds, R., Miller B. Ma, H., Skeen, M., Olds, R., Miller B. and Lauretta, D. S.: Alternative Sample Mass Measurement Technique for OSIRIS-REX Sample Collection Phase, Proceedings of the 44th Annual American Astronautical Society Guidance, Navigation, and Control Conference, 2022
3) May, A., Sutter, B., Linn, T., Bierhaus, B., Berry, K. and Mink, R.: OSIRIS-REx Touch-and-Go (TAG) Mission Design for Asteroid Sample Collection, 65th International Astronautical Congress, Toronto, Canada, 2014.
4) McCann, B.Fagetti, M., McCanna, B.Fagetti, M., Nazari, M., Wittal, M. M. and Smith, J. D.: Mass Property Estimation on TSE(3) via Unscented Kalman Filter Using RCS Thruster. *Acta Astronautica*, **223** (2024), pp. 462-480.
5) McCann, B., Fagetti, M., Nazari, M., Wittal, M. & Smith, J.: Time-varying Mass Property Estimation Utilizing a Joint Unscented Kalman Filter on TSE(3). AAS/AIAA Astrodynamics Specialist Conference, Big Sky, MT. 2023
6) Evans, E.,Evans, E., How, J. P., Thrasher S., & Yang, L. C.: On-Orbit Mass Property Estimation for the Space Shuttle Orbiter with Uncertain Thruster Outputs, AIAA Guidance, Navigation, and Control Conference. AIAA 2018-1603, 2018.